Journal of Structural Geology, Vol. 15, Nos 3–5, pp. 243 to 251, 1993
Printed in Great Britain

0191-8141/93 $06.00+0.00
© 1993 Pergamon Press Ltd

The geometrical classification of folds and distribution of fold types in natural rocks

IVAN S. ZAGORČEV

Geological Institute, Bulgarian Academy of Sciences, 1113 Sofia, Bulgaria

(*Received* 8 *November* 1991; *accepted in revised form* 27 *August* 1992)

Abstract—A further subdivision of fold types 1A and 3 of Ramsay's geometrical classification is proposed. It is based on the occurrence of complementary fold shapes to some of the classes recognized. The parameters of the limiting fold types (1A2, 1B, 2 and 3B) are related to the dip angle by simple equations.

Folds with strongly convergent isogons and thickened limbs (supratenuous folds) of subclass 1A are subdivided into three types, with strongly (1A1), moderately (1A2) and slightly (1A3) thickened limbs, respectively. They commonly develop in diapiric or domal structures due to bending during vertical uplift.

Folds with divergent isogons (class 3) are subdivided into types with slightly (3A), moderately (3B) and strongly (3C) divergent isogons. Folds of subclass 3B are complementary to parallel (subclass 1B) folds; the layers in type 3B folds wedge out at dip angles of 60°, and form complex similar (class 2) folds with adjacent layers folded in type 1B folds. The dominant folding mechanisms related to layer-parallel (or oblique) compression control the thinning in the fold limbs and the formation mainly of folds of types 1B, 1C, 2, 3A and 3B. The extreme types 1A1 and 3C are very rare in natural rocks.

INTRODUCTION

THE development of a geometrical classification of folds based on the shape of a single folded layer in profile section (Ramsay 1967) plays an important role in the quantitative study of fold morphology and in elucidating the principal folding mechanisms. The classification is based on the variations of the relative orthogonal and axial surface-parallel thicknesses and on the dip isogon pattern (Ramsay 1967, pp. 359–372, Hudleston 1973, Ramsay & Huber 1987, pp. 347–363).

Parallel (class 1B) and similar (class 2) folds were the first fold types to be recognized (Van Hise 1896). They are both simple cases, the variation of the layer thickness and the dip isogon angle being described by simple functions of the layer dip angle α. On some forms of graphical representation (Figs. 1–3) these two fold types plot as straight lines separating the fields of the other fold classes and subclasses. The fundamental classes 1 and 3 are characterized, respectively, by convergent and divergent dip isogons, and parallel isogons define similar (class 2) folds (Ramsay 1967). Folds with strongly convergent dip isogons (subclass 1A) were first recognized by Nevin (1931) as supratenuous folds (with decreasing layer thickness in the hinge area), and together with parallel and similar folds they were included in a three-fold classification (Willis & Willis 1934, pp. 34–38).

Analyses of the shapes of folded layers in natural rocks and model materials have demonstrated that some of the fold types are very common whereas others occur only rarely and in very special cases. The extreme fold types in Ramsay's classification (subclass 1A and class 3) show considerable variety, and may be further subdivided on the basis of their geometrical properties and of their frequency of occurrence in natural rocks. The aim of the present paper is to compare the distributions of the different fold types in natural rock sequences, and to propose their further subdivision.

FOLDS WITH STRONGLY CONVERGENT DIP ISOGONS (SUPRATENUOUS FOLDS) (CLASS 1A)

The difference between classes 1 and 3 becomes obvious when comparing the variation of the dip isogon angle φ. Each isogon joins the points on the folded layer surfaces which have the same dip (dip angle α), and the isogon angle is defined as the angle between the isogon and the perpendicular to the tangent to the folded

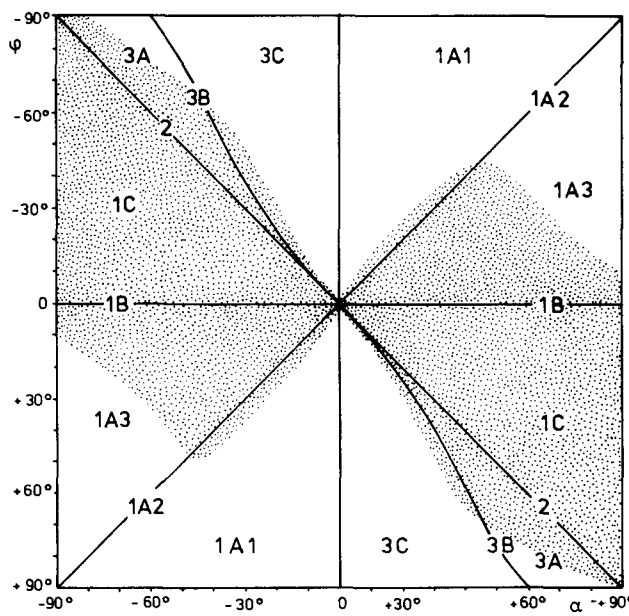

Fig. 1. Plot of the dip isogon angle φ vs the angle of dip α. After Hudleston (1973) with additional subdivision of fold types 1A and 3. The field of fold types most frequent in natural rocks is stippled.

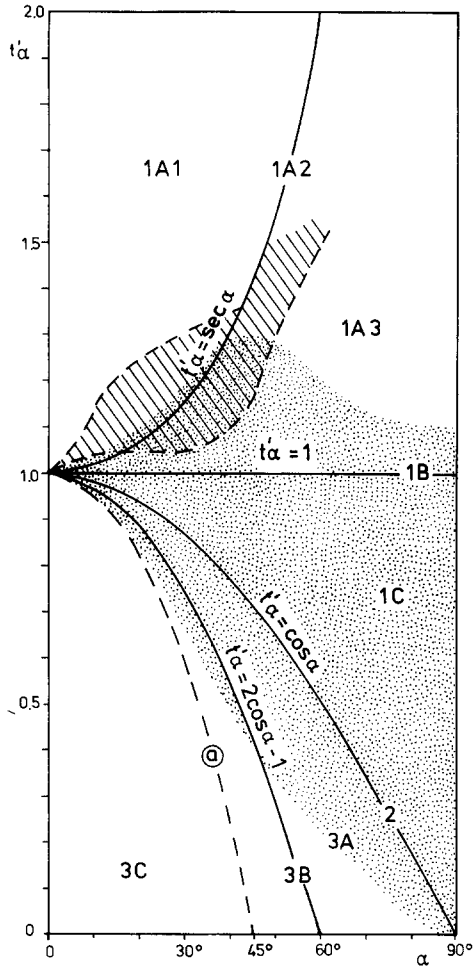

Fig. 2. Plot of orthogonal thickness t'_α vs the angle of dip α. After Ramsay (1967, fig. 7-19) with additional subdivision of fold types 1A and 3. The field of fold types most common in natural rocks is stippled; the field of some diapiric folds is hatched. Curve ⓐ corresponds to

$$t'_\alpha = \frac{2\cos^2\alpha - 1}{\cos\alpha}.$$

surfaces. The sign of the dip isogon angle is defined (Fig. 4) by convention (Hudleston 1973). The majority of natural folds are characterized by a positive dip isogon angle, φ, when the dip angle, α, is positive, and the straight line $\varphi = \alpha$ on Fig. 1 divides two symmetrical fields which correspond to class 3 ($\varphi > \alpha$) and subclass 1C ($\varphi < \alpha$). The field of folds with strongly convergent dip isogons (subclass 1A) is characterized by negative values of φ when α is positive, and remains undivided. However, the geometrical properties of these folds vary considerably, and field 1A may be subdivided in a similar manner to the division of the field of folds with positive dip isogon angles.

If we consider the case $-\varphi = \alpha$, which is symmetrical with respect to $\varphi = \alpha$ (class 2 folds), the relative orthogonal thickness of these 1A folds may be computed as a special case from the expression found by Hudleston (1973)

$$-\varphi = \alpha = \tan^{-1}\left(\frac{1}{t'_\alpha}\frac{\mathrm{d}t'_\alpha}{\mathrm{d}\alpha}\right)$$

or

$$\tan\alpha\,\mathrm{d}\alpha = \frac{\mathrm{d}t'_\alpha}{t'_\alpha} \tag{1}$$

and

$$t'_\alpha = \sec\alpha \tag{2a}$$

$$T'_\alpha = \sec^2\alpha. \tag{2b}$$

Correspondingly (Figs. 1, 2 and 3) subclass 1A may be subdivided (Zagorčev 1974) into three types: 1A1 (with greatly thickened limbs), 1A2 (with moderately thickened limbs) and 1A3 (with slightly thickened limbs).

Most natural class 1A folds belong to type 1A3, close to subclass 1B (Fig. 5). The relative orthogonal and axial-surface parallel thicknesses (Figs. 2, 3 and 5) increase rapidly in the limbs of type 1A2 folds, and the dip isogon becomes perpendicular to the axial surface at a dip angle of 45° (Fig. 5). The formation of type 1A1 folds meets considerable geometrical constraints at higher dip angles. Therefore, the probable range of natural subclass 1A folds is normally limited by the curve $t'_\alpha = \sec\alpha$ (and $T'_\alpha = \sec^2\alpha$) with limb dips usually not exceeding 45°.

FOLDS WITH DIVERGENT DIP ISOGONS (CLASS 3)

Buckled competent layers usually form class 1B (parallel) folds or folds close to 1B of 1A3 or 1C types. An increasing superimposed pure shear ('flattening') component modifies their shapes towards similar (class 2) folds.

The incompetent layers in a multilayer sequence, when buckled, have to accommodate their shape to the shape of the buckled competent layers, forming class 3 folds with divergent dip isogons. The only fold geometry that can penetrate an infinite number of layers is the similar (2) class, and in multilayers the geometries (1C and 3 types) of the individual layers tend to alternate and complement each other in such a manner that the overall geometry is close to the similar type (Ramsay 1967, pp. 430–436). The best and simplest way to subdivide class 3 folds is to find the complementary shape to the pure buckle parallel folds (subclass 1B) of the competent layers.

Let us take a pair of layers of equal thickness (taken as unity). If the pair is folded (Fig. 6) to form a similar (class 2) fold with axial-surface parallel relative thickness $T'_\alpha = 1$ (i.e. with total thickness of the two layers equal to 2), and the competent layer forms a typical parallel fold of 1B type, the variation of T'_α in the incompetent layer may be found by subtracting (from 2.0) the axial-surface parallel thickness of the competent layer, $T'_\alpha = \sec\alpha$, or

$$T'_\alpha = 2 - \sec\alpha. \tag{3}$$

This fold shape corresponds to the curve shown on Fig. 6, and the combination of the two folded layers corresponds to a similar (class 2) fold for dip angles (α)

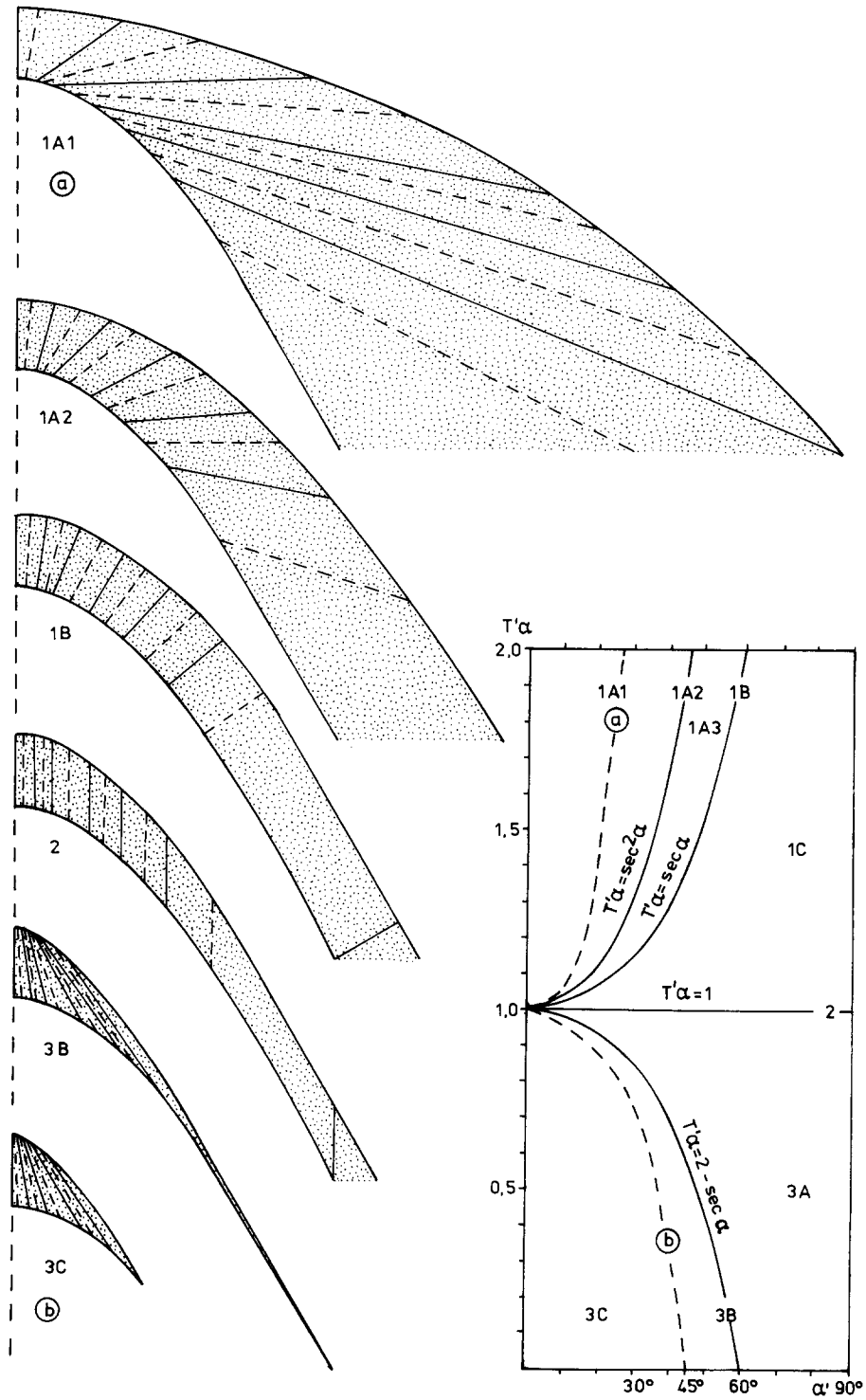

Fig. 3. Profiles of different fold types developed above a sinusoidal single surface with maximum dip angle of 60°. Inset: plot of the thickness parallel to the axial surface T'_α vs angle of dip α (after Ramsay 1967, fig. 7-20), with additional subdivision of fold types 1A and 3. Curve b corresponds to $T'_\alpha = 2 - \sec^2\alpha$.

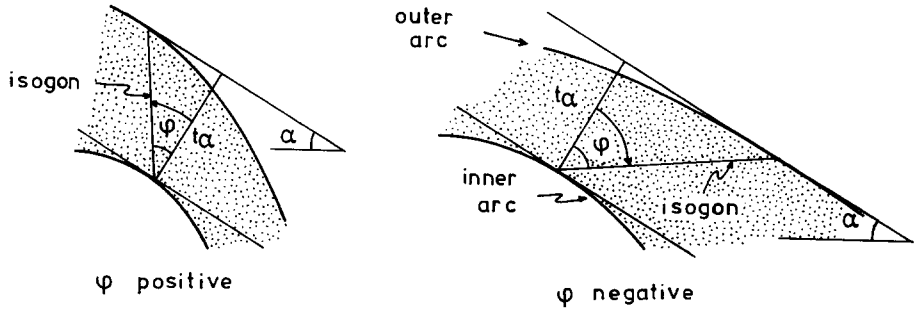

Fig. 4. Sign convention for the dip isogon angle, φ, in the case of a positive dip angle, α (after Hudleston 1973).

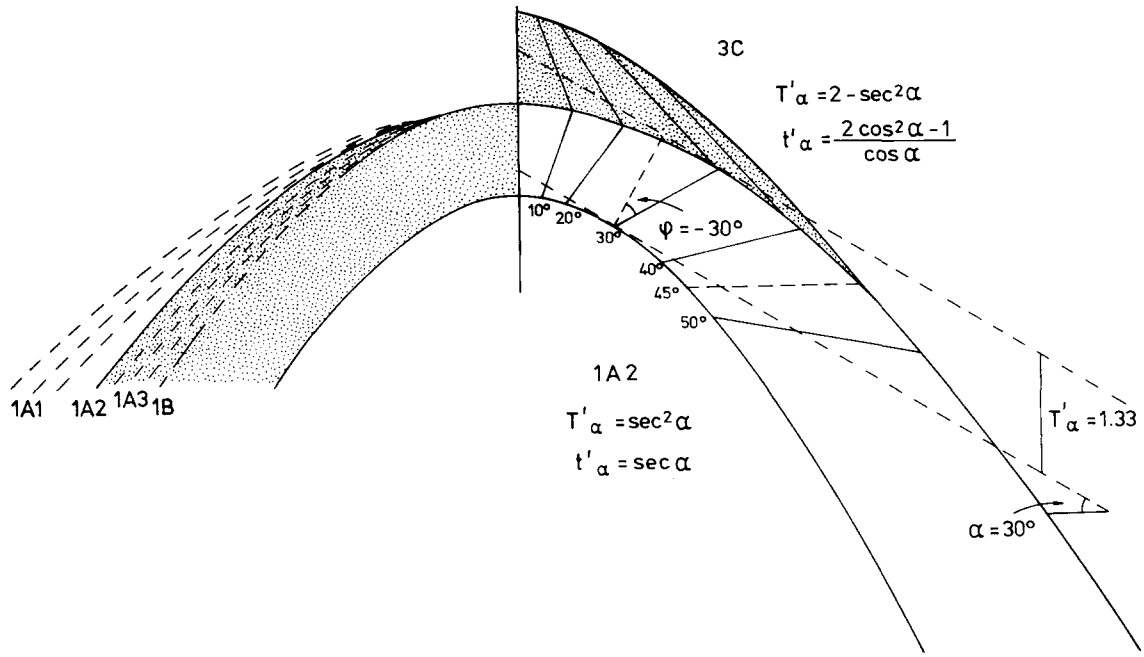

Fig. 5. Profile section of a type 1A2 fold with the position of dip isogons and the complementary type 3C fold (stippled, in the right part) shown. Profile section (stippled, in the left part) of the type 1A2 fold, with possible upper surfaces of types 1A1, 1A3 and 1B folds.

from 0° to 60°. At $\alpha = 60°$ the incompetent layer thins out completely (Ramsay & Huber 1987, p. 358), and this is the limiting curve for the complementary (to subclass 1C) class 3 folds. The curve corresponding to these folds divides the field of class 3 into three subclasses:

—subclass 3A: folds with slightly divergent isogons, $T'_\alpha > 2 - \sec\alpha$;

—subclass 3B: folds with moderately divergent isogons,

$$T'_\alpha = 2 - \sec\alpha, \qquad t'_\alpha = 2\cos\alpha - 1$$

$$\tan\varphi = \frac{\tan\alpha}{2\cos\alpha - 1}; \tag{4}$$

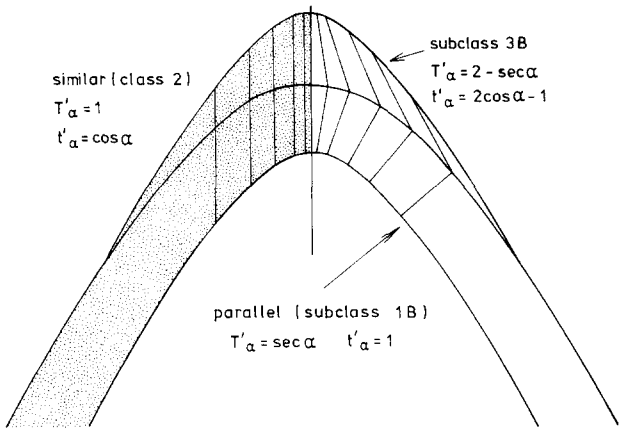

Fig. 6. Profile section of two folds of subclasses 1B and 3B in layers with equal axial-surface parallel thickness, with dip isogons shown for 10, 20, 30, 40 and 50° (in the right part). The two layers complement each other to form a similar fold (stippled) with the dip isogons of a similar fold (left).

—subclass 3C: folds with strongly divergent isogons, $T'_\alpha < 2 - \sec\alpha$.

The parameters of the mutually complementary 1C (with the extreme type 1B) and 3A (with the extreme type 3B) folds may be most readily studied in cuspate–lobate folds.

GEOMETRICAL FEATURES OF CUSPATE–LOBATE FOLDS

Cuspate–lobate folds formed in competent layers tend towards a perfect circular (concentric) shape (subclass 1B) with a maximum layer-parallel shortening of 36% (De Sitter 1956, Ramsay 1967, p. 387), and a wavelength which is close to $W = 2t$. The cusps in the competent layers represent synforms concentrated (in cross-section) at single points on the upper folded boundary, and antiforms concentrated at single points on the lower folded boundary. The points in both cases coincide with the inflexion points. Thus the whole upper boundary consists of lobate antiforms and point-concentrated synforms, and the lower boundary, of lobate synforms and point-concentrated antiforms. Cuspate–lobate folds formed in an incompetent layer of thickness t enclosed in a more competent medium tend to form class 3 folds.

Let us now consider the case (Fig. 7) of perfect cuspate–lobate folds for which the orthogonal thickness of the layer in the axial surface equals $A + nA$ (n may be any number from 0 to infinity). In the case of a competent bed enclosed in an incompetent matrix,

$$t'_\alpha = \frac{1 + n\cos\alpha}{1 + n}, \tag{5}$$

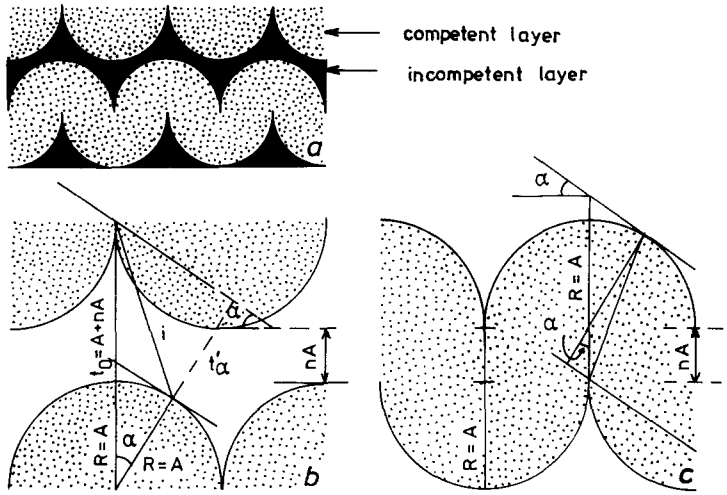

Fig. 7. Profile sections of perfect cuspate–lobate folds, (a) in interlayered competent and incompetent layers, and (b) & (c) showing geometric parameters in the incompetent (b) and competent (c) beds.

and with n approaching zero, t'_α is close to 1, and the folds develop a perfect parallel (concentric) shape (Figs. 7a & c). Increase of n (i.e. increase of the thickness beyond the zone of contact strain influence of the folded boundary) has the same effect as a superimposed pure shear, and as n approaches infinity the effect of $\cos\alpha$ on the expression increases rapidly and the fold geometry becomes close to that of a similar (class 2) fold.

The opposite is observed in perfect cuspate–lobate folds in the incompetent layers (Fig. 7b). The variation of the relative orthogonal thickness is given by

$$t'_\alpha = \frac{(n+2)\cos\alpha - 1}{1+n} \qquad (6)$$

and the perfect cuspate–lobate folds at $n = 0$ correspond to

$$t'_\alpha = 2\cos\alpha - 1.$$

The tangent at $\alpha = 60°$ passes through the cusp point, and the layer is totally reduced with thickness equal to zero.

Increase of n in perfect cuspate–lobate folds (Fig. 8) results in t'_α tending towards $\cos\alpha$, that is the corresponding folds become closer to similar (class 2) folds as in the case of flattening due to superimposed pure shear. This is the field of type 3A folds (with slightly divergent isogons).

Cuspate–lobate folds (including the perfect varieties) are widespread in different geological environments. Examples are found in the quartzo-feldspathic gneissic bands (leptynites) interlayered in migmatitic complexes. Strain partitioning in the competent layers may follow different models. One possibility (Fig. 9) is a combination of a tangential distribution with a neutral surface, and partial flexural flow in the inflexion area. If the neutral surface (or a surface close to it) is marked in the rock in some way, the two parts of the layer may be considered as separate beds forming a composite layer folded in a concentric manner. In this case, the folds in the two beds form shapes complementary to each other (Fig. 10): the upper bed develops a shape close to a type 1A2, and the lower bed a shape with divergent isogons of type 1C but close to a similar (class 2) type at low dip angles. Thus, folds of types 1A2 and 2 complement each other to form folds of type 1B.

POSSIBILITIES FOR FURTHER SUBDIVISION

The geometric classification of folds according to the shape of a single folded layer is based on the recognition of boundary cases in the natural range of geometries and, as for any other classification, it may be regarded as an attempt to find some order in the natural diversity of fold shapes. There is a wide choice of simple functions of the dip angle, α, that could be chosen, but the boundary types already recognized (1A2, 1B, 2 and 3B) seem to be the most appropriate because they represent clearly

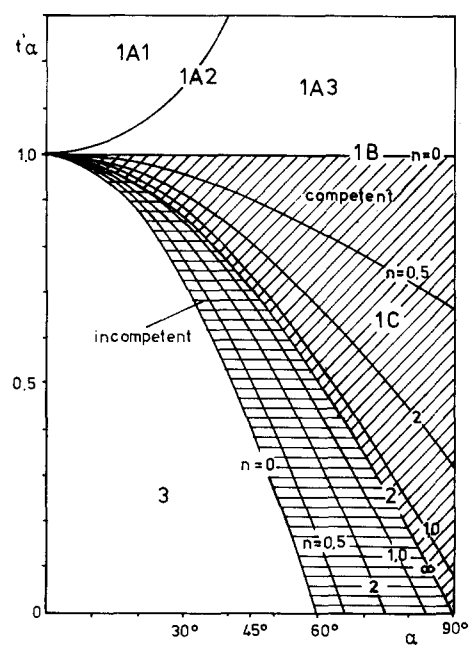

Fig. 8. Variation of t'_α with angle of dip α in perfect cuspate–lobate folds within competent and incompetent layers with different values of parameter n.

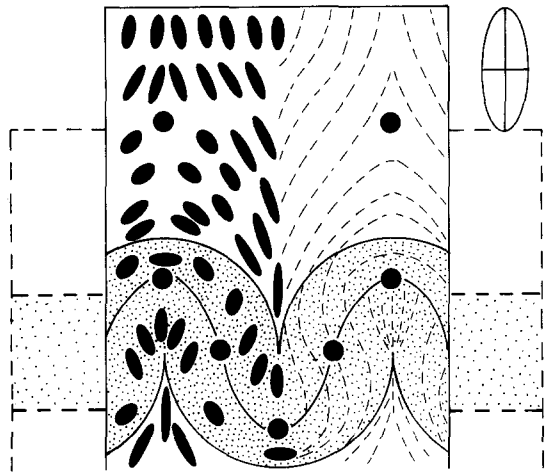

Fig. 9. Possible strain ellipses (left) and trajectories of the X (maximum principal strain) axis (right) in a perfect cuspate–lobate fold in competent (stippled) and incompetent layers folded by a combination of a tangential strain distribution with a neutral surface, and partial flexural flow in the inflexion area.

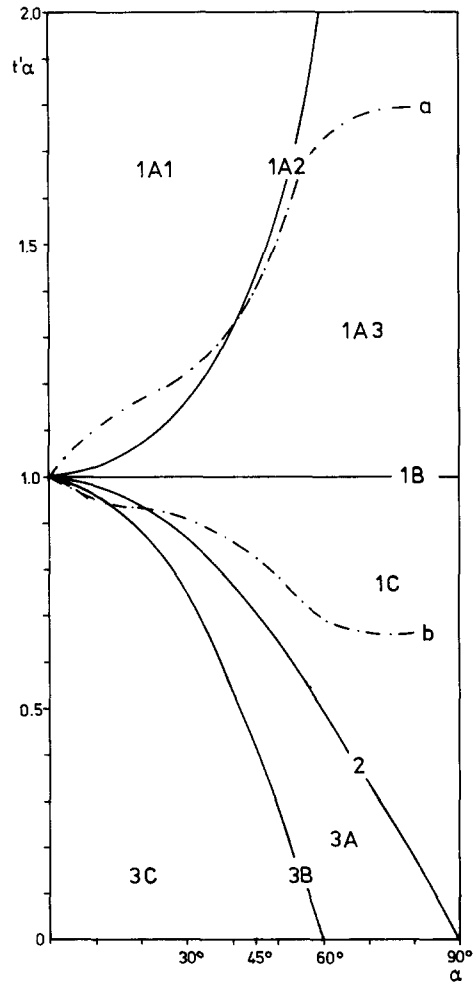

Fig. 10. Variation of t'_α in the fold shown in Fig. 9. The geometry of the folded competent layer is of a concentric (parallel) 1B type. The antiforms in the sublayer above the neutral surface, and the synforms in the sublayer below the neutral surface correspond to a type 1A fold close to 1A2, but beginning in the field of 1A1 and ending in the field of 1A3 (curve a). The synforms above the neutral surface and the antiforms below the neutral surface (curve b) correspond to type 1C folds, but at dip angles from 0 to 30° pass from the field of 3C, close to 3B, through the field of 3A into the 1C field.

defined morphological features which can be easily visualized and characterized. The principle introduced when recognizing the subclass 3B could be applied also to subclass 3C by finding a fold type complementary to type 1A2 (Fig. 5). The variation of T'_α would be given by the function

$$T'_\alpha = 2 - \cos^2 \alpha \tag{7a}$$

and

$$t'_\alpha = 2\frac{\cos^2 \alpha - 1}{\cos \alpha}. \tag{7b}$$

The practical value of such a subdivision of subclass 3C is doubtful. Subclass 1A (supratenuous) folds form in a different folding environment than subclass 3C folds, and alternation of folds of type 1A and 3C to form similar (class 2) compound folds is not likely to occur. Layers corresponding to equations (7a) and (7b) thin out completely at a dip angle of 45° (Figs. 3 and 5), limiting the natural occurrence of such folds.

OCCURRENCE OF DIFFERENT FOLD TYPES IN SOME NATURAL ROCK SEQUENCES

Numerous studies in folded rock sequences have shown the importance of Ramsay's geometrical fold classification, as for example, when discussing the cleavage attitude in folds (Treagus 1982).

The morphological types of folds recognized in natural rocks depend largely upon the folding mechanisms involved. Therefore, many authors have tried to introduce a combined classification, sometimes confusing geometrical and genetic properties.

Mechanisms of folding (Van Hise 1896, Ramberg 1961, 1963, Donath & Parker 1964, Ramsay 1967, Ramsay & Huber 1987) are usually related either to buckling under conditions of layer-parallel (or at an oblique angle) shortening or to axial-surface parallel shear and slip. Both mechanisms form periodic folds and lead to thinning of the layers in the fold limbs with respect to the hinges. These processes may be amplified by a superimposed homogeneous 'flattening' strain.

Although a special case, cuspate–lobate folds are widespread (Ramsay 1967, Ramsay & Huber 1987) in different geological environments. They are formed by the buckling of multilayers with a competence contrast between the adjacent layers, and very often at the boundaries between comparatively rigid basement and ductile cover. These mechanisms favour the development of fold types 1B, 1C, 2, 3A and 3B. A folding mechanism of lesser importance is the bending of overlying layers by rising diapirs, granite domes, rigid basement blocks (stamp folds), etc. This process favours the development of subclass 1A (mainly 1A3 to 1A2) folds (Fig. 11).

In a number of morphological fold types, such as chevron folds, the folds become 'locked' (Ramsay 1967, pp. 436–456) at a given dip angle (most commonly, *ca*

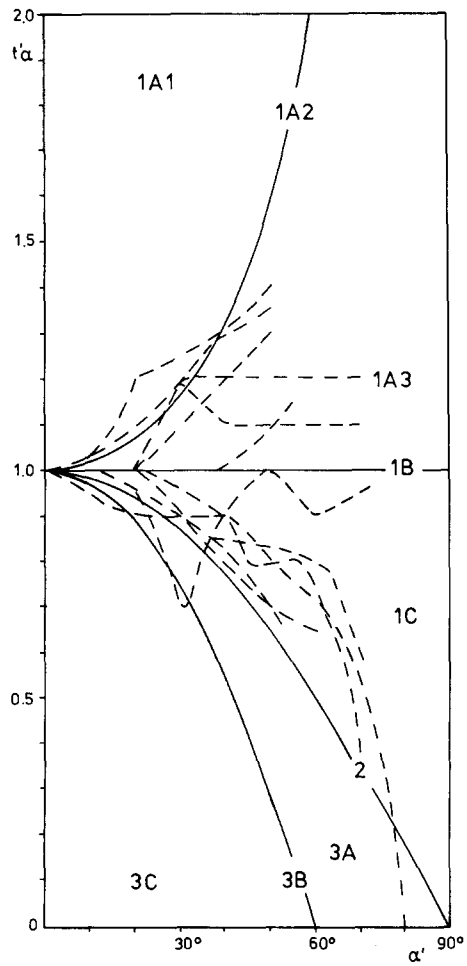

Fig. 11. Variation of t'_α with α in folds above a diapir (natural examples and model experiments).

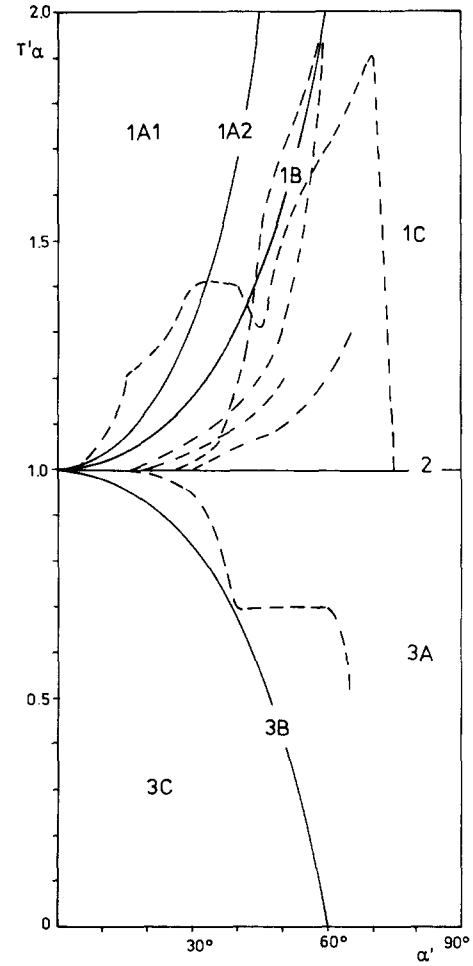

Fig. 12. Variation of T'_α with α in Cambrian red slates, Dinorwic Quarry, North Wales.

60°) of the folded layer. A similar locking mechanism may be expected also for the isogon angle, φ, which rarely is higher than 45° (especially in the 1A folds).

The purple slates in the Cambrian slate belt of North Wales possess a considerable thickness and homogeneity. The folds often show (Fig. 12) alternating type 1C and 3A shapes, although the competence difference between adjacent layers is usually very low.

Folds in the red beds of the Permian Skrino Formation and the Lower Triassic Marvodol Formation in southwest Bulgaria (Fig. 13) belong to subclass 1C and (partially) to subclass 3A. The formations consist of alternating competent and incompetent layers, in the basal parts of the Marvodol Formation with a predominance of competent quartz conglomerates and sandstones. The Upper Triassic red beds of the Komštica Formation are dominated by incompetent layers, and are highly strained due to Late Triassic and Mid Cretaceous folding and thrusting. Correspondingly, folds of subclasses 1C and 3A (close to class 2) occur with almost equal frequency.

The development of folds in migmatized gneiss–amphibolite complexes (e.g. in the Rhodope Massif, the Ograždden block of southwest Bulgaria, etc.) leads to particularly complicated layer morphologies (Fig. 14). Besides the alternation of folds of subclasses 1C and 3A typical of multilayers with beds of different rheological properties, some folds are characterized by a rapid decrease of layer thickness at dip angles between 30° and 50° in such a manner that class 1 folds change to type 3A, and type 3A folds become modified into types 3B or 3C. In the limbs near the inflexion points, at dip angles between 50° and 70°, the layer thickness increases, and the fold type returns to the character it has in the hinge area. Possible variations of this kind are, for example (with increasing dip angle α):

1A–1B–1C–1B–1A;
1A–1B–1C–2–3A–2–1C;
1C–2–3A–3B–3C–3B–3A.

Such changes may be analysed (Ramsay 1967, pp. 365–371) in terms of the variation of the rate of change of t'_α with dip angle α ($dt'_\alpha/d\alpha$), and even of the variation of the second derivative of the relative orthogonal thickness t'_α with α. The structure of a fold very similar to that shown by curve a in Fig. 14 may be classified accordingly as a divergent isogon fold compounded with a convergent (1A) isogon fold (Ramsay 1967, figs. 7-27 and 7-28, table 7-4). Natural reasons for such a variation may be sought in: (i) primary changes in layer thickness; (ii) changes in the competence contrast (relative rheology)

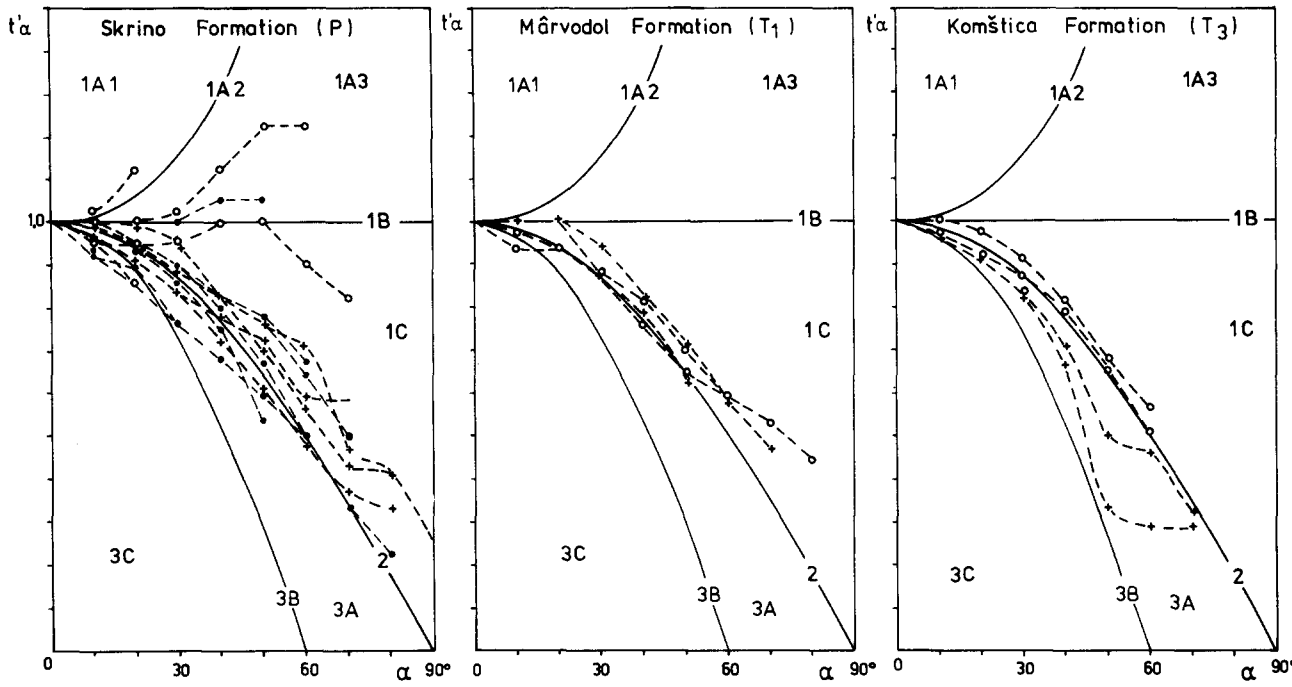

Fig. 13. Variation of t'_α with α in Permian and Triassic red beds in southwest Bulgaria.

Table 1. Geometrical classification of folds (after Ramsay 1967), with additional subdivision of types 1A and 3 based on layer thickness distribution and dip isogons

Fold type	Dip isogons	Layer thickness in the limbs	Variation of φ	Variation of t'_α	Variation of T'_α
Class 1	Convergent		$\varphi < \alpha$	$t'_\alpha > \cos\alpha$	$T'_\alpha > 1$
1A (supratenuous)	Strongly convergent	Increasing	$\varphi < 0$	$t'_\alpha > 1$	$T'_\alpha > \sec\alpha$
1A1		Strongly increasing	$-\varphi > \alpha$	$t'_\alpha > \sec\alpha$	$T'_\alpha > \sec^2\alpha$
1A2		Moderately increasing	$-\varphi = \alpha$	$t'_\alpha = \sec\alpha$	$T'_\alpha = \sec^2\alpha$
1A3		Slightly increasing	$-\varphi < \alpha$	$\sec\alpha > t'_\alpha > 1$	$\sec^2\alpha > T'_\alpha > \sec\alpha$
1B (parallel)	Moderately convergent	Constant orthogonal thickness t	$\varphi = 0$	$t'_\alpha = 1$	$T'_\alpha = \sec\alpha$
1C	Slightly convergent	Slightly decreasing without wedging	$\alpha > \varphi > 0$	$1 > t'_\alpha > \cos\alpha$	$\sec\alpha > T'_\alpha > 1$
Class 2 (similar)	Parallel	Constant axial-surface thickness T	$\varphi = \alpha$	$t'_\alpha = \cos\alpha$	$T'_\alpha = 1$
Class 3	Divergent	Decreasing with wedging	$\varphi > \alpha$	$\cos\alpha > t'_\alpha$	$1 > T'_\alpha$
3A	Slightly divergent	Wedging at $\alpha > 60°$	$\tan\varphi < \frac{\tan\alpha}{2\cos\alpha - 1}$	$\cos\alpha > t'_\alpha > 2\cos\alpha - 1$	$1 > T'_\alpha > 2 - \sec\alpha$
3B	Moderately divergent	Wedging at $\alpha = 60°$	$\tan\varphi = \frac{\tan\alpha}{2\cos\alpha - 1}$	$t'_\alpha = 2\cos\alpha - 1$	$T'_\alpha = 2 - \sec\alpha$
3C	Strongly divergent	Wedging at $\alpha < 60°$	$\tan\varphi > \frac{\tan\alpha}{2\cos\alpha - 1}$	$2\cos\alpha - 1 > t'_\alpha$	$2 - \sec\alpha > T'_\alpha$

due to changes in the *P–T* conditions; (iii) simple shear in the fold limbs at critical values (30–50°) of the dip angle; (iv) redistribution of mobile components (quartz, K-feldspar, etc.) during the several superimposed folding events; and (v) a selective response to pure shear. Evidence for these kinds of processes has been found in all migmatitic terrains studied, and the development of a fold or fold set commonly continues through several metamorphic events under considerable changes in *P–T* conditions and rheologic behaviour of the rocks.

CONCLUSIONS

The occurrence of the various fold types of the geometrical fold classification (Figs. 1, 2 and 3, Table 1) in many sedimentary and metamorphic complexes is controlled mainly by the folding mechanisms most common under natural conditions. The newly-proposed subclasses 1A2 and 3B, together with the well-known parallel (subclass 1B) and similar (class 2) types are limiting fold shapes which correspond to simple functions of the dip angle. They separate the other fold types, which

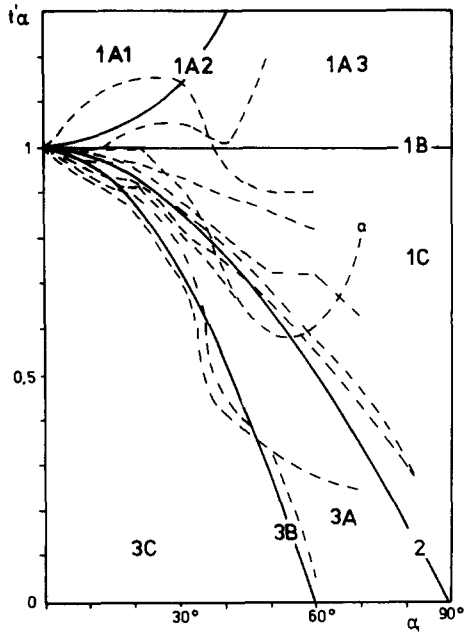

Fig. 14. Variation of t'_α with α in folded migmatites and amphibolites of the Ograzdenian Supergroup, southwest Bulgaria. Curve a is discussed in the text.

have more variable parameters. The formation of the extreme types 1A1 and 3C is unlikely to occur under natural conditions, and may be expected only in very rare cases, at low to moderate dip angles. Compound folds with changing layer morphology are usually related to a change in the strain field and in the rheologic behaviour during several deformational events which have modified the primary fold shape.

Acknowledgements—This paper was largely inspired by the M.Sc. course given by J. G. Ramsay many years ago. Thanks are due to the reviewers Richard Lisle and Brian Chadwick and to Dorothee Dietrich for valuable suggestions which contributed both to the better representation of the content and to the improvement of the English.

REFERENCES

De Sitter, L. U. 1956. *Structural Geology*. McGraw-Hill, New York.

Donath, F. A. & Parker, R. B. 1964. Folds and folding. *Bull. geol. Soc. Am.*, **75**, 45–62.

Hudleston, P. J. 1973. Fold morphology and some geometrical implications of theories of fold development. *Tectonophysics* **16**, 1–46.

Nevin, C. M. 1931. *Principles of Structural Geology*. J. Wiley & Sons, New York.

Ramberg, H. 1961. Relationships between concentric longitudinal strain and concentric shearing strain during folding of homogeneous sheets of rocks. *Am. J. Sci.* **259**, 382–390.

Ramberg, H. 1963. Strain distribution and geometry of folds. *Bull. geol. Inst. Univ. Uppsala* **42**, 1–20.

Ramsay, J. G. 1967. *Folding and Fracturing of Rocks*. McGraw-Hill, New York.

Ramsay, J. G. & Huber, M. I. 1987. *The Techniques of Modern Structural Geology, Volume 2: Folds and Fractures*. Academic Press, London, 309–700.

Treagus, S. H. 1982. A new isogon-cleavage classification and its application to natural and model fold structures. *Geol. J.* **17**, 49–64.

Van Hise, C. R. 1896. Deformation of rocks. *J. Geol.* **4**, 449–483, 593–629.

Willis, B. & Willis, R. 1934. *Geologic Structures* (3rd edn). McGraw-Hill, New York.

Zagorčev, I. 1974. Some problems of classification and terminology of folds. *Rev. Bulg. geol. Soc., Sofia* **35**, 338–343 (in Bulgarian).